FIRST PRINCIPLES STUDY OF THE ELECTRONIC STRUCTURE OF Al/Ti:ZnO CRYSTAL

R. Plugaru[a)] and N. Plugaru[b,c)]

[a)]National Institute for R&D in Microtechnologies-IMT Bucharest, PO-BOX 38-160, 023573 Bucharest, Romania
E-mail: rodica.plugaru@imt.ro
[b)]Dpto. Ciencia y Tecnologia de Materiales y Fluidos, Centro Politecnico Superior (CPS), Universidad de Zaragoza, 50018 Zaragoza, Spain
[c)]National Institute of Materials Physics, P.O.Box MG-07, Bucharest-Magurele 77125, Romania

Abstract

We present results of ab initio calculations in the Local (Spin) Density Approximation, L(S)DA, of the electronic structure of Al and Ti doped ZnO crystal. Whereas both dopants modify the density of states at the Fermi energy, the structure and population of the impurity band is different in the two cases. Our results predict a non magnetic ground state for Al doped ZnO crystal, with the concentration x(Al)= 2-20 at.%. In the case of Ti doping the calculations predict a magnetic ground state and we obtain a magnetic moment localized on Ti ion of 1.14, 1.20, 1.28 and 1.54 μ_B/Ti ion for x(Ti) = 2, 5, 10 and 20 % , respectively. We discuss the results in terms of the carriers role in the interplay between conductivity and magnetism in these materials.

***Keywords**: Al/Ti-doped ZnO, electronic structure, L(S)DA calculations, diluted magnetic smiconductors*.

1. INTRODUCTION

Zinc oxide (ZnO) has been investigated as an excellent candidate for fabrication of transparent conducting films used in optoelectronics, in photovoltaic devices and flat panel displays. The advantages of ZnO include a relatively easy lithography processing and low cost raw material. As well, ZnO thin films have emerged as materials with a great potential of improvement of their properties, e.g. the conductivity and the transparency in the visible range [1-3]. A resistivity lower than 1×10^{-4} Ω·cm was recently reported for ZnO thin films doped with Al and a transmittance exceeding 90% [4]. Recently, we have witnessed a constantly growing interest in using the spin coherence of electrons in addition to their charge in information technology [5]. Basic requirements for the operation of the so-called spintronic devices are: i) a high spin polarization current; ii) high spin diffusion length, and iii) the integration of spin detection device. Several classes of magnetic materials are investigated for their use in spin-electronics, including: i) diluted magnetic semiconductors (doped with nd transition metal or rare earths ions, or engineered to exhibit d0 magnetism), ii) the Heusler alloys [6] or other half-metallic ferromagnets [7,8], and iii) the semimagnetic semiconductors which exhibit the property of giant Zeeman-splitting [9]. Among these materials, the diluted magnetic semiconductors (DMS), and therefore doped ZnO, are particularly attractive due to their reported room temperature ferromagnetism and compatibility with the silicon technology [10, 11]. On the theoretical side, detailed investigations of the dopant effect on the electronic structure of ZnO have been carried out in order to understand the dopant effect on the conduction states [12-15].

In this contribution we present results of a first principles study of the electronic structure in Al and Ti doped ZnO crystal. We assumed the substitutional character of Al and Ti doping and the wurtzite-type (B4) structure, space group P63mc, in the investigated impurity concentration range, x= 2-20 at.%.

2. COMPUTATIONAL METHODOLOGY

We carried out self consistent scalar-relativistic calculations in the Local (Spin) Density Approximation, L(S)DA, using the FPLO (version 5.00–20) band structure code [16]. FPLO is an all-electron code based on the method of linear combination of non-orthogonal local orbitals. The overlap of the basis functions ensures the coverage of the whole space and a high degree of adaption. The basis sets used in the present calculations were: i) for Zn(Ti)

3s3p:4s4p3d;5s5p4d, ii) for O 1s:2s2p;3s3p3d, and iii) for Al 2s2p:3s3p;4s4p3d corresponding to semicore: valence; polarization states, respectively. Basis optimization was achieved for each concentration, independently. The site-centered potentials and densities were expanded in spherical harmonic contributions up to l_max=12. We used the exchange and correlation potential in the parameterization of Perdew and Wang [17]. A Brillouin zone sampling with a 16×16×16 k-mesh ensures an accuracy of 10^-5 eV in the total energy and is sufficient to deal with Fermi surface effects for the metallic phases resulting from electron doping. The disordered systems are treated in the Coherent Potential Approximation (CPA) using the multiscattering formalism of Blackman-Esterling-Berk implemented in the FPLO scheme [18]. In this approach, the atomic centers are distributed on periodic lattice points where the atomic potential is site-dependent. FPLO uses Mulliken population analysis which works satisfactorily in the case of minimal basis sets and covalent compounds, as is the case of ZnO. We carried out the calculations at the experimental lattice constants [19] and neglected the lattice relaxation since we are interested in pure substitutional effects of the dopants on the band structure.

3. RESULTS AND DISCUSSION

The DOS plot of the pure, non defective ZnO, shown in Figure 1, exhibits the main features as obtained with other LDA calculations [20]. The LDA-LCAO band gap is 0.94 eV (whereas the experimental one is 3.4 eV). The valence band has a width of approximately 5.5 eV and shows the strong overlap between Zn(3d) and O(2p) states. The localized Zn(3d) states are centred at about -8 eV. The CB consists of two regions: a lower one of mainly Zn(4s) states and a higher one of Zn(4p) states. Al and Ti substitution for Zn leads to the appearance of donor states in the system. The valence band shifts to lower energy, a density of states, $N(E_F)$, arises at the Fermi level and increases with the dopant concentration, see the total density of states ploted in Figures 2 and 3. More details on the evolution of the band structure as a result of Al and Ti doping may be observed in the element-

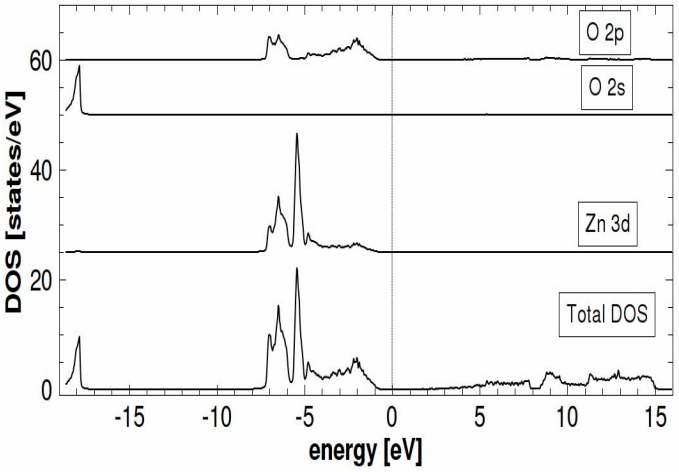

Fig.1. Total, element and l-projected DOS of ZnO. Zn 3d, O2s and 2p states are shifted on the y axies for visibility. The Fermi level is set at 0 energy.

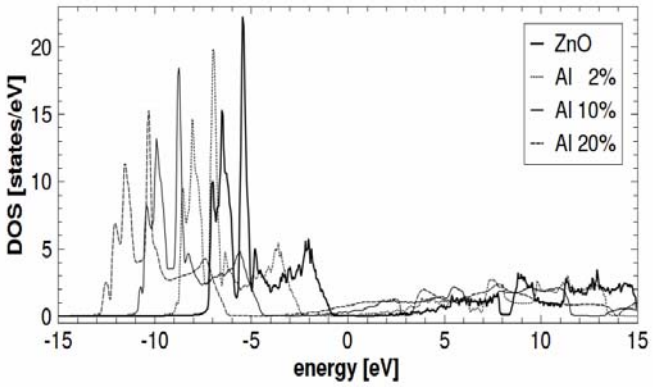

Fig. 2. Total DOS of ZnO doped with x= 2, 10 and 20 % Al. DOS of pure ZnO is also shown. The Fermi level is set at zero energy.

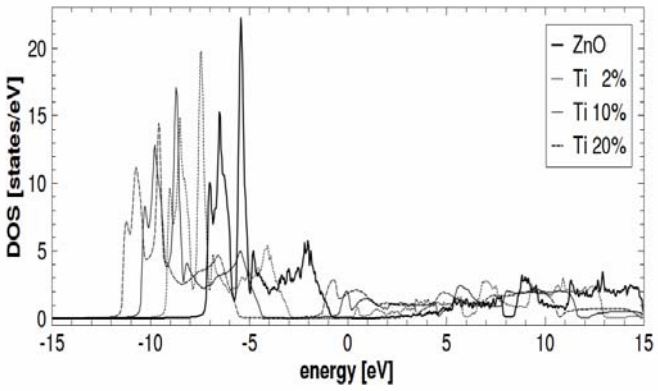

Fig. 3 Total DOS of ZnO doped with x= 2, 10 and 20 % Ti. DOS of pure ZnO is also shown. The Fermi level is set at zero energy.

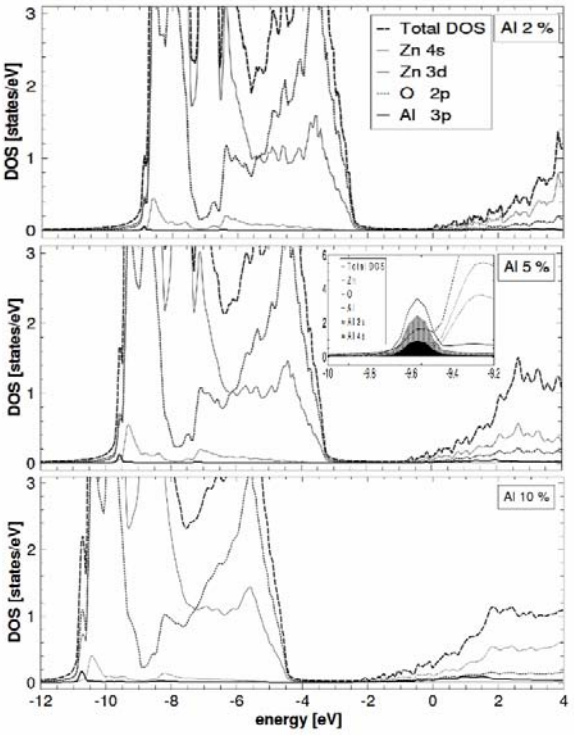

Fig.4 Total DOS and element and l-projected DOS of ZnO doped with: i) 2 % Al top panel, ii) 5 % Al middle panel and iii) 10 % Al bottom panel. Inset middle panel: Enlarged image of the valence band bottom showing Al 3s and 4s states. Note that the Al states are scaled.

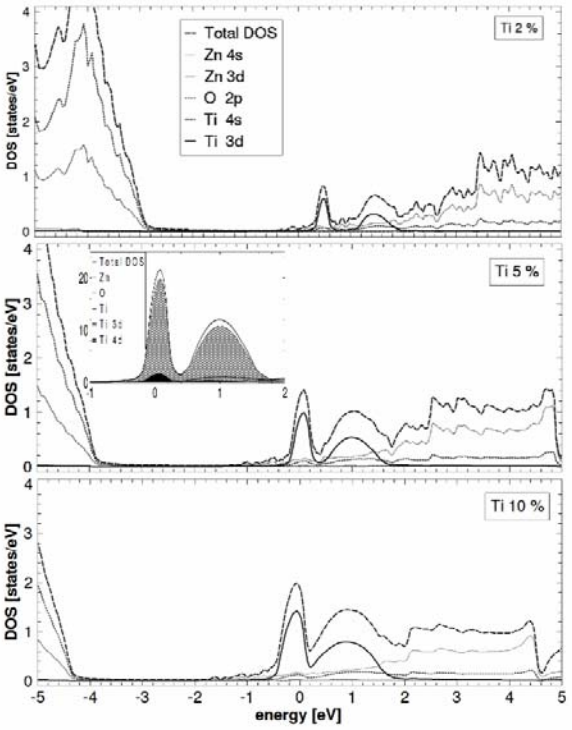

Fig.5 Total DOS and element and l-projected DOS of ZnO doped with: i) 2 % Ti top panel, ii) 5 % Ti middle panel and iii) 10 % Ti bottom panel. Inset middle panel: Enlarged image of the Fermi level region showing Ti 3d and 4d states. Note that the Ti states are scaled.

In the case of Al, see Figure 4, $N(E_F)$ increases slowly, from 0.02 states/eV for 2% Al, to 0.21 states/eV for 10% Al and to 0.75 states/eV for 20% Al. The Fermi level shifts to higher energy, from -0.70 eV for 2% Al to 1.24 eV for 20% Al. The N(EF) is low, as well as the number of carriers in the CB and one should not expect a significant increase in the electrical conductivity at Al doping less than approx. 5 %. Al(3s) states, mainly, and Al(4s) states, secondarily, contribute to a narrow band localized at the bottom of the VB, see Inset in Figure 4.b, as an example for 5% Al.

Experimentally, it has been determined that Al doped ZnO films can reach resistivities as low as $1.4\times10^{-4}\Omega\cdot$cm to $2.9\times10^{-4}\Omega\cdot$cm [21]. Several groups also investigated the effect of Ti and a value of $3.82\times10^{-3}\Omega\cdot$cm was reported (see [22] and the references cited therein). The decrease in resistivity was attributed to an increase in the free carriers concentration. A semiconductor-metal transition was also reported in [23]. The LDA results for Ti doping show a peak in the density of states at the Fermi level, due to Ti(3d) states, mainly, and also Ti(4d) states, secondarily, see Figure 5; these states also contribute to a peak situated at approx. 1 eV in the CB, see Inset in Figure 5.b. $N(E_F)$ shows a variation determined by the shift of the Fermi level toward the CB; thus, $N(E_F)$ increases uniformly from 0.04 states/eV for 2% Ti, to 1.93 states/eV for 10% Ti, then decreases to 1.16 states/eV for 15% Ti and increases again to 1.87 states/eV for 20% Ti.

Our results predict a non magnetic ground state for Al doped ZnO, derived from a comparison of total energy in spin unpolarized and spin polarized calculations, in consistency with reported results. In the case of Ti doping the impurity band at the Fermi level is exchange split and the calculations predict a magnetic ground state, in agreement with previous experimental [24] and first principles [25] results. We summarize in the Table the spin magnetic moment on Ti and the magnetic moment per formula unit at several Ti concentrations. Previously, it has been established that carrier-

mediated ferromagnetism is responsible for the magnetism of diluted magnetic semiconductors (DMS) [26].

Table. *The magnetic moment per Ti ion and the magnetic moment per formula unit.*

Ti(at.%)	μ(Ti)(μ_B/at.)	M(μ_B/f.u.)
2	1.14	0.023
5	1.20	0.063
10	1.28	0.133
20	1.54	0.327

In order to interpret their experimental findings, i.e. a magnetic moment of 2.6μ_B and 0.5μ_B per dopant atom for 5% Co- and Ti-containing ZnO, respectively, [24], Coey *et al.* have proposed a model which assumes that the exchange is mediated by carriers in a spin-split impurity band derived from extended donor orbitals [27]. Our present results of first principles calculations, which predict magnetism in Ti doped ZnO crystal, are in conceptual agreement with the model [27].

Both Al and Ti contribute charge carriers to the system and therefore the doped ZnO undergoes a transition semiconductor - material with metallic type electrical conductivity, when the dopant concentration increases. The LSDA results also support the onset of a magnetic moment on Ti as a result of the impurity band exchange splitting at the Fermi level. LSDA+U (U= local Coulomb repulsion) calculations are underway in order to get a more accurate picture of the electronic structure and magnetism in disordered Ti:ZnO crystal. Based on the calculated electronic structure data we discuss the role of the carriers in the exchange split impurity band in the conduction and magnetic properties.

4. CONCLUSIONS

Al and Ti doping of ZnO crystal determines an evolution of the band structure at the Fermi level from that of a semiconductor to that characteristic for metallic conduction. Nevertheless, there are significant diferences between the Al and Ti systems. The details of the changes in the electronic structure at the Fermi energy indicate a non magnetic ground state for Al doping and possible ferromagnetism in the case of Ti doping. A rough estimation of the magnetic ordering temperature in Ti:ZnO by converting the total energy difference in spin-unpolarized and spin-polarized calculations yields the values 60 K, 188 K and 385 K for x(Ti)= 2%, 5% and 10%, respectively. The calculated magnetic moment per Ti ion rises a question on the Ti configuration in Ti:ZnO.

Acknowledgments

This work was supported by Project 11-048/2007-2010 NANOXI, funded by the National Authority for Scientific Research, Romania. The authors acknowledge with thanks the support received from Ulrike Nitzsche and ITF Dresden on issues related to using the computational cluster and FPLO code.

5. REFERENCES

[1] I. Volintiru, M. Creatore, M. C. M. Van Sanden, In stiu spectroscopic ellipsometry growth studies on the Al-doped ZnO films deosited by remote plasma-enhanced metalorganic chemical vapor deposition, J. Appl. Phys. 103, pp.033704-1-10 (2008).

[2] X. Wang, Q. Lei, W. Xu, W. Zhou, J. Yu, Preparation of ZnO:Al thin films on transparent TPT substrate at room temperature by RF magnetron sputtering technique, Matterials Letters 63, pp.1371-1373 (2009).

[3] S. D. Kirby, R.B. van Dover, Improved conductivity of ZnO through codoping with In and Al, Thin Solid Films 517, pp. 1958-1960 (2009).

[4] D.-J. Kwak, M. W. Park, Y.-M. Sung, Discharge power dependence of structural and electrical properties of Al-doped ZnO conducting film by magnetron sputtering (for PDP), Vacuum 83, pp. 113-118 (2009).

[5] D.D. Awschalom and N. Samarth, Spin dynamics and quantum transport in magnetic semiconductor quantum structures, J. Magn. Magn. Mat. 200 (1999) 130.

[6] I. Galanakis, P. H. Dederichs and N. Papanikolaou, Slater-Pauling behavior and origin of the half-metallicity of the full-Heusler alloys, Phys. Rev. B 66, p.174429 (2002).

[7] K.P Kamper, W. Schmitt, G. Guntherodt, R.J. Gambino and R. Ruf, CrO_2 - A New Half-Metallic Ferromagnet ?, Phys. Rev. Lett. 59, p. 2788 (1988).

[8] J.-H. Park, E. Vescovo, H.-J. Kim, C. Kwon, R. Ramesh, and T. Venkatesan, Nature (London) 392, p. 794 (1998).

[9] R. Fiederling, M. Keim, G. Reuscher, W. Ossau, G. Schmidt, A. Waag, and L.W. Molenkamp, Injection and detection of a spin-polarized current in a light-emitting diode, Nature (London) 402, p.787 (1999).
[10] H. Ohno, Toward Functional Spintronics, Science 291, p. 840 (2001).
[11] S.A. Wolf, D.D. Awschalom, R.A. Buhrman, J.M. Daughton, S. von Molnar, M.L. Roukes, A.Y. Chtchelkanova, D.M. Treger, Spintronics: A Spin-Based Electronics Vision for the Future, Science 294, p. 1488 (2001).
[12] P. Palacios, K. Sanchez, P. Wahnon, Ab-initio valence band spectra of Al, In doped ZnO, Thin Solid Films 517, pp.2448-2451 (2008).
[13] D. Iusan, R. Knut, B. Sanyal, O. Karis, O. Eiksson, Electronic Structure and chemical and magnetic interactions in ZnO doped with Co and Al: Experiments and ab initio density-functional calculations, Phys. Rev. B 78, pp. 085319-1-9 (2008).
[14] S. Z. Karazhanov, P. Ravindran, A. Kjekshus, H. Fjellvag, B.G. Svensson, Electronic structure and optical properties of ZnX (X=O, S, Se, Te): A density functional study, Phys. Rev. B 75, pp. 155104 (2007).
[15] N. A. Spaldin, Search for ferromagnetism in transition-metal-doped piezoelectric ZnO, Phys. Rev. B 69, p. 125201 (2004).
[16] K. Koepernik and H. Eschrig, Full-potential nonorthogonal local-orbital minimum-basis band-structure scheme, Phys. Rev. B 59, pp. 1743-1757 (1999).
[17] J. P. Perdew, Y. Wang, Accurate and simple analytic representation of the electron-gas correlation energy, Phys. Rev. B 45, pp. 13244-13249 (1992).
[18] K. Koepernik, B. Velický, R. Hayn and H. Eschrig, Self-consistent LCAO-CPA method for disordered alloys, Physical Review B 55, pp. 5717-5729 (1997).
[19] T. M. Sabine and S. Hogg, Acta Cryst. B 25, pp. 2254 (1969).
[20] A. Janotti, C.G.Van de Walle, New insights into the role of native point defects in ZnO, J. Criystal Growth 287, p. 58 (2001).
[21] K. Ellmer, Resistivity of polycrystalline zinc oxide films: current status and physical limit, J. Phys. D: Appl. Phys. 34, pp. 3097-3108 (2001).
[22] Y. R. Park, K. J. Kim, Optical and electrical properties of Ti-doped ZnO films: observation of semiconductor–metal transition, Solid State Communications 123, pp. 147-150 (2002).
[23] J.J. Lu, Y.M. Lu, S.I. Tsai, T.L. Hsiung, H.P. Wang, L.Y. Jang, conductivity enhancement and semiconductor-metal transition in Ti-doped ZnO films, Optical materials 29, 1548-1552 (2007).
[24] M. Venkatesan, C. B. Fitzgerald, J.G. Lunney and J.M. D. Coey, Anisotropic Ferromagnetism in Substituted Zinc Oxide, Phys. Rev. Lett. 93, pp.177206-4 (2004).
[25] K, Osuch, E.B. Lombardi, W. Gebiski, First principles study of ferromahnetism in $Ti_{0.0625}Zn_{0.9375}O$.
[26] H. Ohno, Properties of ferromagnetic III-V semiconductors, J. Magn. Magn. Mat., 200, pp.110-129 (1999).
[27] J. M. D. Coey, M. Venkatesan and C. B. Fitzgerald, Donor impurity band exchange in dilute ferromagnetic oxides, Nature Materials 4, pp. 173 (2005).